Penerbit Akademia Baru

Journal of Advanced Research Design

Journal homepage:
https://akademiabaru.com/submit/index.php/ard
ISSN: 2462-1943

Effect of Lithium Doping Concentration on Morphology, Structural, Optical and Electrical Properties of Cu_2O Thin Films

Nur Nisha Najjini[1], Mohd Zamzuri Mohamad Zain[1,*], Mahyiddin Mohamed[2], Marina Marzuki[2], Fariza Mohamad[3], Pei Loon Khoo[4]

[1] Faculty of Mechanical Engineering Technology, Universiti Malaysia Perlis (UniMAP), Pauh Putra Campus, 02600 Arau, Perlis, Malaysia
[2] Faculty of Electronic Engineering Technology, Universiti Malaysia Perlis, Pauh Putra Main Campus, 02600, Arau, Perlis, Malaysia
[3] Faculty of Electrical & Electronic Eng., University Tun Hussein Onn Malaysia, 86400, Parit Raja, Batu Pahat, Johor, Malaysia
[4] Department of Mechanical Eng., Toyohashi University of Technology, 1-1 Hibari Gaoka, Tempaku, Toyohashi, Aichi 441-8580, Japan

ARTICLE INFO

Article history:
Received 17 January 2025
Received in revised form 14 February 2025
Accepted 2 June 2025
Available online 13 June 2025

Keywords:
Cuprous oxide; Li doped Cu_2O; Electrodeposition

ABSTRACT

Oxide thin-film photovoltaic devices are promising for renewable energy applications due to their low material usage, inexpensive manufacturing potential, and low electrical resistivity. The variation of lithium concentration shows significant effect on the Cu_2O layer properties. The morphology, structural, optical and electrical properties of the Cu_2O thin films were investigated. As the result, by using the variation of lithium doping concentration. Li doped Cu2O thin films with high crystallinity combined with optical and optimal electrical properties can be synthesized. Lithium doping with 0.15 M, results obtained compact structure with crystallite that were 53.11 nm in sizes, and superior electrical properties for carrier concentration and resistivity with value of carrier concentration at 3.78 x 10^{21} /cm^3 and resistivity at 5.58 x 10^{-5} Ω.cm respectively. The findings suggest that Li doping can be an effective strategy to improve the performance of photovoltaic devices by reducing resistivity and increasing carrier concentration while potentially enhancing charge carrier transport within the material.

1. Introduction

Cuprous oxide (Cu_2O) is regarded as a promising p-type semiconductor material in photovoltaics, photocatalysis, and optoelectronics due to its stability, ease of preparation, abundance in nature, non-toxicity, and visible-light activity with a direct bandgap of 2.0~2.6 eV [1- 3]. Cu_2O is a metal oxide semiconductor material with a cubic crystal structure. It is a p-type semiconductor material with a lot of application in solar cells. Copper oxide thin films have been made using a variety of physical and chemical processes including nebulizer pyrolysis [4], thermal oxidize copper sheet [5], magnetron sputtering [6,7], spin coating [8], and electrodeposition [9,10] method have recently been reported. Electrochemical deposition is one of the most basic and low-cost techniques: it is adaptable and highly efficient for large-area device production [11]. Furthermore, the electrochemical parameters

* *Corresponding author.*
E-mail address: mzamzuri@unimap.edu.my

https://doi.org/10.37934/ard.134.1.8898

and the composition of the electrolytic solution can be tweeted, providing for greater control over the film thickness, morphology, and nature of the thin films produced, making electrodeposition more desirable. Moreover, single-phase Cu_2O thin films can be produced by changing all electrodeposition parameters [12].

Furthermore, the smaller grain size of the Cu_2O oxide thin film may alter electron transportation, leading to recombination loss before an electron enters the excited state, which directly reduces the efficiency of the photovoltaic device [13]. Lachinov *et. al* also discovered that doping the element in the Cu_2O thin films increased the electrical conductivity along the interface greatly, not by raising the concentration of charge carriers, but by increasing their mobility [14]. The microstructure also can be altered by doping with several elements. In addition, doping in cuprous oxide with insoluble impurities of dopant in thin film solar cells increases the potential of turning its energy band gap [15,16] and also can change the microstructure of the thin film.

In this work, we investigate the functional properties of undoped and Li doped Cu_2O thin films with variety of doping concentrations by electrodeposition method. We offer a thorough investigation of the morphological, structural, optical, and electrical characteristic of undoped and Li doped Cu_2O thin films using a variety of specialized characterization techniques, including FESEM, AFM, XRD, UV-Vis, and HALL Effect measurement. Our research has shown that controlling the doping concentration during deposition is essential for achieving the best possible thin film physical characteristics.

2. Methodology

2.1 Preparation of ITO Substrate Glass

The ITO glass (~10 mΩ) with dimension of 2 cm x 1 cm x 0.75 mm (l x w x t) was chosen as a substrate. Before the electrodeposition procedure, the ITO glass was split into two areas; deposited and non-deposited area, and then soaked in acetone for around 2 minutes (min). The glass substrate was then rinsed with deionized water before being dried with pressurized air.

2.2 Electrodeposition Undoped and Li Doped Cu_2O Thin films

The electrodeposition of Cu_2O thin films was performed in a two-electrode, with a Pt wire as the counter electrode and ITO substrate glass as the working electrode. A platinum wire is used as an anode since it cannot be oxidized as a cathode. The Cu_2O electrolyte solution was made by dissolving 79.86 g of 99 % copper (II) acetate monohydrate ($C_4H_{10}CuO_6$) (Kanto Chemical Co., Inc.), 270.24 g of 85~92 % lactic acid ($C_3H_6O_6$) (Kanto Chemical Co., Inc.), and 210 g potassium hydroxide, KOH (Kanto Chemical Co., Inc.) with chemical purity 86 % into 500 ml of ultrapure water (UPW) at ambient temperature. All aqueous solutions used here were prepared with a water purification system by a Milli-Q IQ 7003. The pH of the solution was adjusted to 12.5 by adding KOH. The deposition parameters for the electrodeposition process are shown in Table 1. In starting solution for Li doped Cu_2O thin films, 95% pure magnesium hydroxide (Acros Organics) was formulated as 0.05 M, 0.10 M, 0.15 M, and 0.2 M of Li doping on Cu_2O.

Table 1
Electrodeposition parameter undoped and Li doped Cu_2O

Deposition parameters	Values
Current (mA)	2.0
Voltage (V)	1.0
Bath temperature (^oC)	45.5
Solution temperature (^oC)	40.0
pH value	12.5
Deposition time (min)	3.0

2.3 Characterization of Analysis

The morphology of undoped Cu_2O and Li doped Cu_2O on ITO glass substrate was observed by FESEM (Leo 1525) with 20x to 70x magnification and 7 kV of accelerating voltage. Next, the optical properties of thin films were observed by UV-Vis (Perkin ELMER LAMBDA 950 Series) in the wavelength range of 200-800 µm referenced to the air. For electrical properties of thin film were observed by HALL Effect Measurement (ECOPIA HT55T3) with current 5 mA, and diameter 0.1 µm to measure the carrier concentration, mobility carrier, and resistivity.

3. Results

3.1 The Appearance of Undoped and Li Doped Cu_2O Thin Films

The schematic illustration of Li doped Cu_2O on ITO substrate is shown in Figure 1. The Cu_2O layer was deposited on ITO substrate with different concentrations of 0.05 M, 0.10 M, 0.15 M, and 0.2 M Li. Figure. 2 depicts the physical appearance of Cu_2O layer before and after doping with various concentration of Li. After depositing undoped and Li doped Cu2O on the clear ITO substrate, the color changes to a homogeneous light brown. There are no discernible differences in the appearance of Cu_2O thin films with increasing Li doping concentrations.

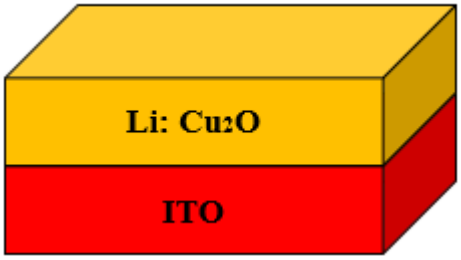

Fig. 1. Illustration cell configuration of Li doped Cu_2O on ITO substrate glass

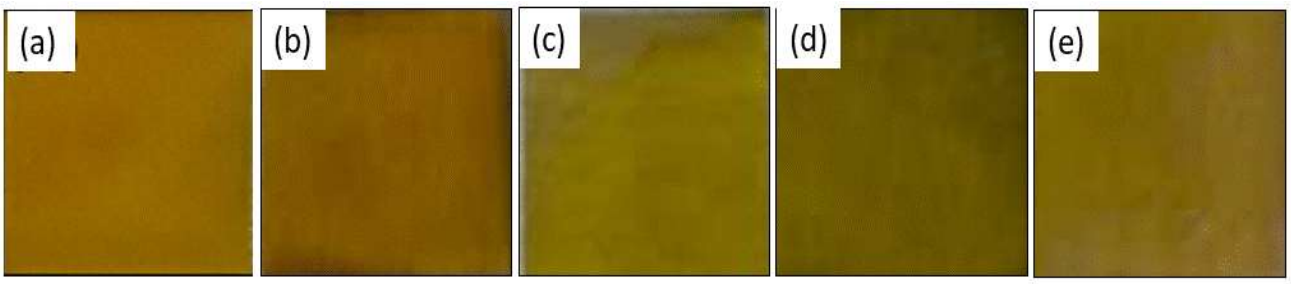

Fig. 2. The appearance of (a) undoped, (b) 0.05 M, (c) 0.10 M, (d) 0.15 M, and (e) 0.20 M Li doped Cu_2O

3.2 Surface Morphology of Undoped and Li Doped Cu_2O Thin Films

The surface profile directly affected the property of materials and was an important parameter. Therefore, to observe the shape evolution of morphologies of Cu_2O microcrystals. Figure 3 shows the morphology of undoped Cu_2O thin film. The Cu_2O grains show a pyramid-like structure with an apparent uniform and compact. Figure 4 shows the morphology of Li doped Cu_2O thin films with different dopant concentrations. The Li doped Cu_2O grains show a porous pyramid shape with an apparent uniform structure. The grain size change within the among of doping concentration. The pyramid shape with uniform structure was observed at 0.05 M, 0.10 M, and 0.20 M Li doped Cu_2O, while 0.15 M shows the structure with porous structure and pyramid shape of Cu_2O was changed to another shape like a sphere. The explanation was that the stress existed in the grains that changed the structure of grains after doped with Li [16].

3.3 Structural Properties of Undoped and Li Doped Cu_2O Thin Films

The crystal structure and orientation of Li doped Cu_2O on ITO substrate glass were investigated using X-ray diffraction (XRD). Figure 5 shows the XRD patterns for the deposited Cu_2O layer with different concentrations of Li doping. The deposited Cu_2O thin films revealed orientation which was indexed to (111) at 36.4^o of diffraction peak, with secondary peak corresponding to the (200) reflection at 43.0^o of diffraction peak for all doping concentrations on the Cu_2O layer. The Cu_2O orientation was corresponding to the cubic pattern (PDF 01-071-3645). Whilst, the peak for CuO could be seen after doping on the Cu_2O layer. The peak of CuO was indexed to (002) at 35.5^o of diffraction peak. The additional peak of CuO compound (202) at 47.3^o is observed for undoped, 0.05 M, 0.10 M, and 0.15 M Li doped Cu_2O. The CuO region was existed due to the voltage that used in electrodeposition process that was mentioned in table Cu_2O water system. No other peaks related to Li phases was found, indicating that secondary phases were not present in the produced thin films.

Additionally, with doping concentrations between 0.05 M and 0.20 M, the (111) and (200) peaks in the undoped and Li doped Cu_2O thin films exhibit a substantial increase in intensity. We detect a sharp decline in crystallinity, as shown for the thin films produced at 0.10 M, as shown by a reduction in the intensity of the (111) peak and the highest peak of (002). A 3 x 3 x 3 Mg doped Cu_2O supercell's ionic relaxation produced a theoretical XRD pattern that, it should be emphasized, is well congruent with the peak locations [17].

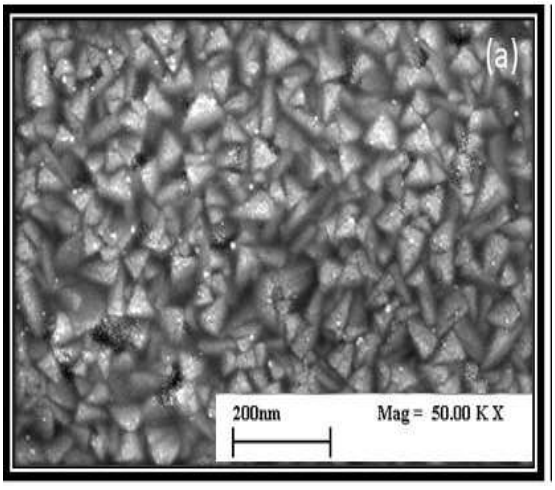

Fig. 3. Morphology structure of undoped Cu_2O by FESEM

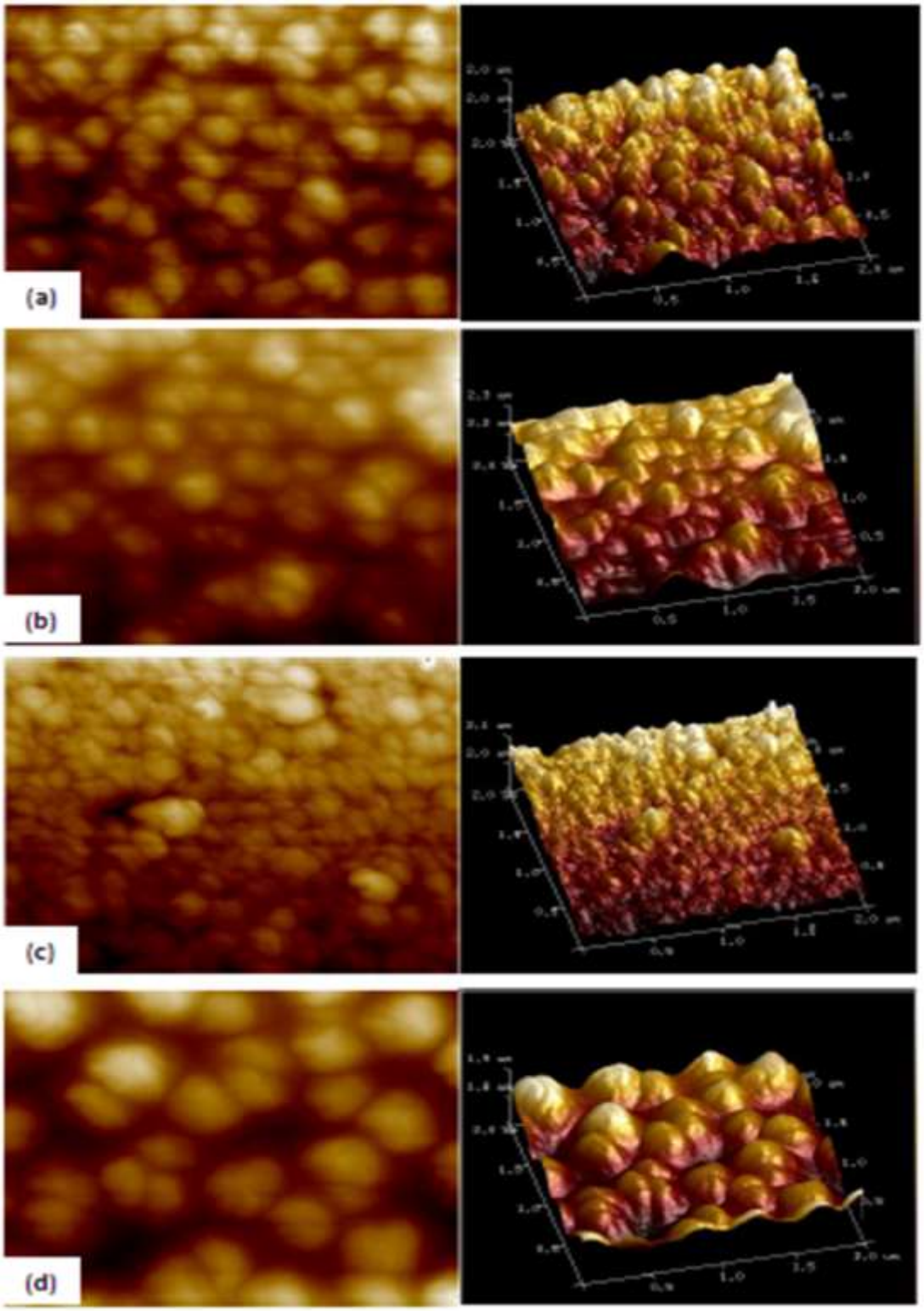

Fig. 4. Average grain size of (a) 0.05 M, (b) 0.10 M, (c) 0.15 M, and (d) 0.20 M Li doped Cu_2O

In addition, the crystallite size was obtained from the analysis of the X-ray Diffractometer using Scherrer's Eq. (1) [18],

Scherrer Formula $D = \frac{K\lambda}{\beta \cos \theta}$ (1)

Where, the Scherrer constant is -D, the wavelength of XRD is -λ, the FWHM -β, and the peak position -θ. Table 1 shows the size of the crystallites from 0.05 until 0.15 M decreased from 43.98 nm to 25.87 nm and then increased to 42.26 nm at 0.2 M. The effect of the lithium content seems especially visible in the layer, 0.1 M of Li, where the crystallite size compatible with the observations by AFM shows that the grains are more compact than other concentrations.

3.4 Optical Analysis of Undoped Cu_2O and Li Doped Cu_2O Thin Films

The optical parameter of all the samples was observed in the range of 300 to 800 nm at room temperature as shown in Figure 6. The Cu_2O layer exhibited an absorption edge around 600 nm, the interference fringe pattern was clearly detected at wavelength around 600 nm, confirming the production of a homogenous Cu_2O layer with a distinctive bandgap energy of 2.1 eV [19]. At wavelength of 500 nm, the higher absorption was obtained by 0.1 M Li doped Cu_2O, followed by undoped, and other concentration which are 0.05 M, 0.15 M and 0.2 M. Absorption performance mainly depends on certain factors, such as lattice strain, film thickness, insufficient oxygen, and particle size of the samples [20]. The lithium incorporation inside the Cu_2O lattice structure establishes an impurity level (acceptor level) above the valance band. As the concentration of impurities increased the wavefunction of electrons bound to the impurity atoms starts to overlap and then forms an energy band rather than a discreet impurity level and then can enhance the absorption coefficient. The all absorbance of visible light shows the same pattern for undoped and Li doped Cu_2O.

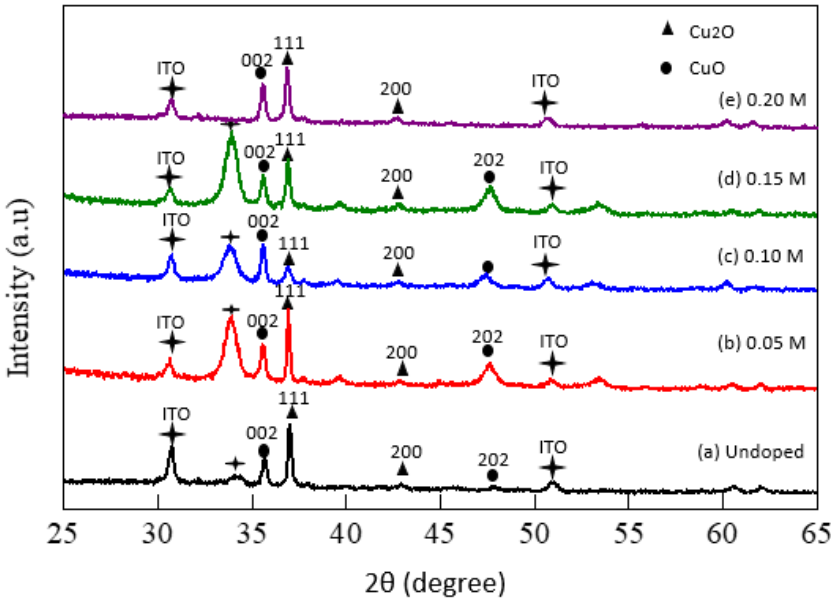

Fig. 5. XRD pattern of undoped and Li doped Cu_2O thin films

As shown in Table 2, following the Li doping, a decrease of the band gap value with respect to undoped Cu_2O thin film is reported. This observation can be put into perspective with the lower absorbance values obtained with the lower doping concentration. However, as Li doping into Cu_2O, the band gap increases from 2.10 eV to 2.45 eV at 0.15 M Li doped Cu_2O. The widening of the band gap of the thin films could be attributed to the Moss–Burstein effect (also known as Bur- stein–Moss shift, or BM shift) linked to the high carrier concentration leading to the degeneration of the semiconductor. This phenomenon gives rise to an increase of the apparent band gap value. Therefore, in our work, the change of the optical bandgap of the Cu_2O thin films with the Li doping concentrations could be triggered by the increase of the carrier concentration [21,22].

Table 2
Average grain size, crystallite size, and band gap of undoped and Li doped Cu_2O

Samples	Dopant concentration (M)	Average Grain size (nm)	Crystallite size (nm)	Energy band gap
a	Undoped	84.18	41.78	2.10
b	0.05	245.29	87.79	2.30
c	0.10	231.24	42.38	2.25
d	0.15	157.12	53.11	2.45
e	0.20	375.41	57.45	2.41

The optical band gap energy (Eg) of the undoped and Li doped thin films were calculated from the absorption spectra using the variation of the absorption coefficient (α) with photon energy according to the following Eq. (2),

$$(\alpha hv)^{1/p} = A(hv - E_g) \quad (2)$$

Where, E_g is the optical band gap, A is a constant, h the Planck constant, v the frequency of the incident photons, and exponent p is the transition probability. For p=1/2, the transition is direct and allowed; for p = 2, it is indirect and allowed, and for p = 3/2, it is direct and forbidden. The values of the optical energy gap were estimated by extrapolation of the linear portion of the graph plotted between hv and (αhv).

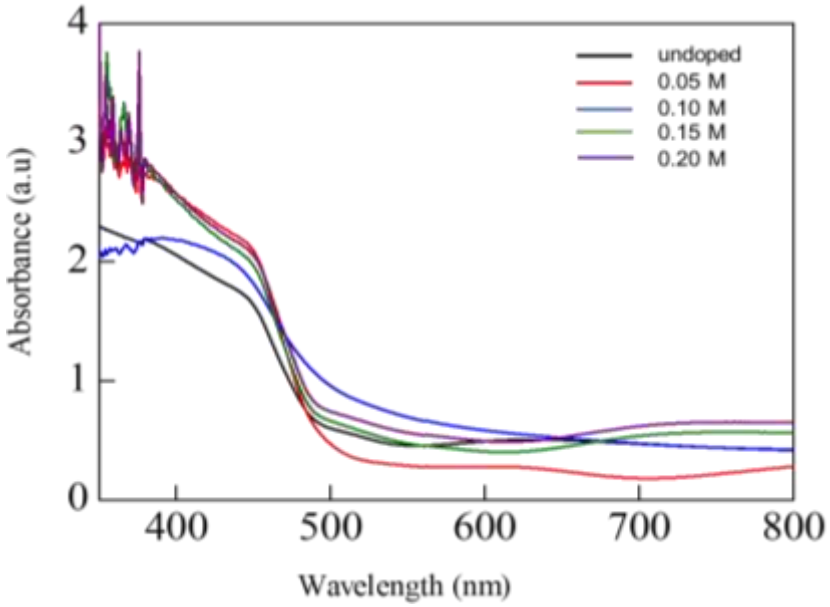

Fig. 6. Absorption spectrum of undoped and Li doped Cu_2O thin films

3.5 Electrical Analysis of Undoped and Li Doped Cu_2O Thin Films

The carrier concentration, mobility carrier, and resistivity of electrodeposited undoped and Li doped Cu_2O thin films were analysed using Hall effect measurement. Table 3 shows the result of Hall effect measurement of the undoped and Li doped Cu_2O.

An electrical characterization by Hall effect measurements was conducted to determine carrier concentration, mobility, and sample resistivity shown in Figure 7. These parameters play a crucial role in determining the material's conductivity and overall electrical performance. First, it is important to note that all Cu_2O thin films have a p-type semiconducting characteristic. The findings provide insights into the potential suitability of Li doped Cu_2O thin films for specific electronic or

magnetic device applications. In a study by Nyborg *et al.*, [24] highly doped Cu_2O films showed a significant decrease in resistivity by three orders of magnitude. However, this decrease in resistivity was accompanied by a decrease in carrier mobility. The presence of high Li content in the samples was discovered to passivate acceptor states generated from copper vacancies, raising carrier concentration [23]. These results align with the current study, where Li doping exhibited similar effects on resistivity and mobility, with the sample doped at 0.2 M Li concentration showing the optimal values in both parameters [24]. The carrier mobility decreases as a result of this, but mobility greater than 10 cm^2/Vs is maintained in all samples. One possibility for the rise is that Li passivates a compensatory donor in Cu_2O. This would explain why the apparent carrier concentration increased at room temperature. Furthermore, Li doping in Cu_2O could lead to the emergence of further unidentified flaws.

Overall, the comparison with these studies supports the notion that Li doping has a significant influence on the electrical properties of semiconducting materials. The differences in mobility carrier, carrier concentration, and resistivity observed in the current study align with the findings of previous research. The electrical characterization validates the pattern that was previously mentioned and highlighted in the analysis of the structural properties of the thin films. The increase in electrical conductivity is likely brought about by the Li doped Cu_2O thin films improved crystalline quality and compact grain sizes. The fewer pores, which act as traps for free holes and barriers for hole transport in thin films, are produced by the larger and more compact grain size. As a result, an increase in the size of the grains and a decrease in porosity lead to an increase in overall electrical conductivity [25]. This is further supported by the improvement in crystallinity that the XRD data indicated.

In our study, the layer deposited with 0.15 M Li doping has the highest grains quality with the lowest resistivity value of 5.58 x 10^{-5} Ωcm, corresponding to a highest charge carrier concentration 3.78 x 10^{21} cm^{-3} and lowest mobility carrier 2.96 cm^2/vs, respectively. According to findings from earlier studies, the reduced hole mobility with increasing plasma pressure may be directly related to increased charge carrier dispersion brought on by an increase in defect concentration [26] . We also note that the resistivity of the undoped and Li doped thin films achieved lowest than other researchers which is by a factor negative 5.

Table 3
Analysis result of HALL effect measurement of the undoped and Li doped Cu_2O

Concentration of Li doping (M)	Carrier concentration x 10^{21} ($/cm^3$)	Mobility carrier x 10 (cm^2/vs)	Resistivity x 10^{-5} (Ωcm)
Undoped	3.01	3.56	5.83
0.05	2.92	3.57	5.98
0.10	3.48	3.17	5.66
0.15	3.78	2.96	5.58
0.20	2.97	3.59	5.87

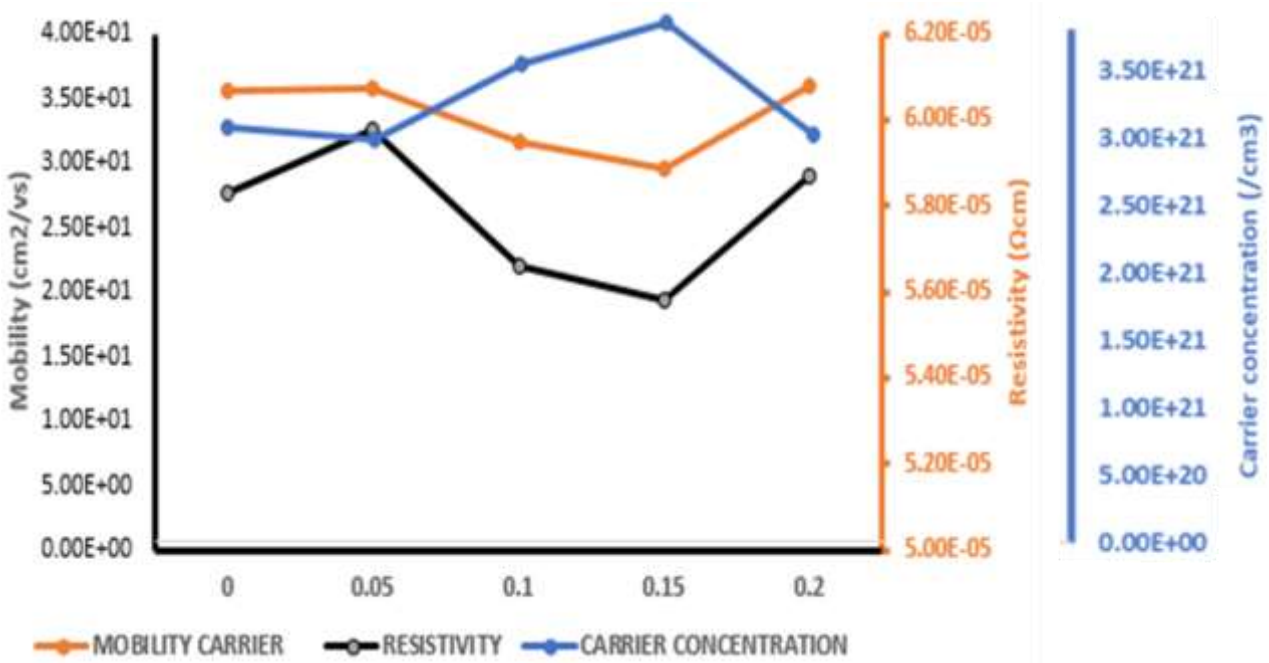

Fig. 7. Carrier concentration, mobility, and resistivity for undoped, 0.05 M, 0.10 M, 0.15 M and 0.2 M Li doped Cu_2O

4. Conclusions

The Li doped Cu_2O/ITO was created through the electrodeposition of a p-Cu_2O layer on the ITO substrate followed by the formation of doping Li at various concentrations. The Cu_2O layer was formed on an ITO substrate using an electrodeposition method in an alkaline aqueous solution containing copper (II) acetate and lactic acid. The structural result shows that Li doped Cu_2O films possess a pyramid structure and polycrystalline nature with (111) and (200) preferred orientation, and the formation (002) and (202) of CuO were observed. AFM revealed that increasing the dopant concentration changed the grain size of the structure due to stress that existed in the crystals after Li doped Cu_2O. The Hall Effect results showed that Li doped Cu_2O improved the electrical characteristics of Cu_2O at certain concentrations in terms of bulk concentration, mobility, and resistivity with 0.15 M Li doped Cu_2O showing superior electrical properties for carrier concentration and resistivity with value of carrier concentration at 3.78 x 10^{21} /cm^3 and resistivity at 5.58 x 10^{-5} Ω.cm respectively. The findings highlight the potential of p-Li doped Cu_2O thin films to enhance photovoltaic device performance. Further research is recommended to evaluate the performance and stability of these thin films in actual device structures. Optimization of doping concentration and deposition parameters can be explored for even better performance. Long-term stability studies under different environmental conditions would provide insights for practical applications. Furthermore, investigating the influence of other doping elements, such as Sodium or Aluminum, on the electrical and optical properties of Cu_2O thin films can contribute to a better understanding of their impact on device performance. These advancements can lead to more efficient and sustainable renewable energy generation systems.

Acknowledgement

The author gratefully acknowledges the financial support provided by the Malaysian Ministry of Higher (MOE) through the Fundamental Research Grant Scheme (FRGS) under Grant No. FRGS/1/2019/TK07/UNIMAP/02/2.

References

[1] Zainal, S. M., M. Zamzuri, M. Hasnulhadi, Z. Nooraizedfiza, M. Marina, Fariza Mohamad, N. Hisyamudin, and M. Izaki. "Effect of annealing temperature on construction of CuO layer on electrodeposited-Cu2O layer by annealing." In IOP Conference Series: Materials Science and Engineering, vol. 429, no. 1, p. 012097. IOP Publishing, 2018. https://doi.org/10.1088/1757-899X/429/1/012097

[2] Zhao, Ying-jie, Yan Li, Yong-bin Wu, Wei Zhou, and Fu-xin Zhong. "Preparation and photoelectric properties of praseodymium-doped cuprous oxide thin films." Journal of Materials Science: Materials in Electronics 31 (2020): 3092-3100. https://doi.org/10.1007/s10854-020-02855-4

[3] Yue, Yamei, Pengxin Zhang, Wei Wang, Yuncheng Cai, Fatang Tan, Xinyun Wang, Xueliang Qiao, and Po Keung Wong. "Enhanced dark adsorption and visible-light-driven photocatalytic properties of narrower-band-gap Cu2S decorated Cu2O nanocomposites for efficient removal of organic pollutants." Journal of hazardous materials 384 (2020): 121302. https://doi.org/10.1016/j.jhazmat.2019.121302

[4] Jacob, S. Santhosh Kumar, I. Kulandaisamy, S. Valanarasu, A. M. S. Arulanantham, V. Ganesh, S. AlFaify, and A. Kathalingam. "Enhanced optoelectronic properties of Mg doped Cu 2 O thin films prepared by nebulizer pyrolysis technique." Journal of Materials Science: Materials in Electronics 30 (2019): 10532-10542. https://doi.org/10.1007/s10854-019-01397-8

[5] Mittiga, Alberto, Enrico Salza, Francesca Sarto, Mario Tucci, and Rajaraman Vasanthi. "Heterojunction solar cell with 2% efficiency based on a Cu2O substrate." Applied physics letters 88, no. 16 (2006). http://iopscience.iop.org/1882-0786/8/2/022301

[6] Noda, S., H. Shima, and H. Akinaga. "Cu2O/ZnO heterojunction solar cells fabricated by magnetron-sputter deposition method films using sintered ceramics targets." In Journal of Physics: Conference Series, vol. 433, no. 1, p. 012027. IOP Publishing, 2013. https://doi.org/10.1088/1742-6596/433/1/012027

[7] Gan, J., V. Venkatachalapathy, B. G. Svensson, and E. V. Monakhov. "Influence of target power on properties of CuxO thin films prepared by reactive radio frequency magnetron sputtering." Thin Solid Films 594 (2015): 250-255. https://doi.org/10.1016/j.tsf.2015.05.029

[8] Oku, Takeo, Tetsuya Yamada, Kazuya Fujimoto, and Tsuyoshi Akiyama. "Microstructures and photovoltaic properties of Zn (Al) O/Cu2O-based solar cells prepared by spin-coating and electrodeposition." Coatings 4, no. 2 (2014): 203-213. https://doi.org/10.3390/coatings4020203

[9] Hussain, Sajad, Chuanbao Cao, Ghulam Nabi, Waheed S. Khan, Zahid Usman, and Tariq Mahmood. "Effect of electrodeposition and annealing of ZnO on optical and photovoltaic properties of the p-Cu2O/n-ZnO solar cells." Electrochimica Acta 56, no. 24 (2011): 8342-8346. https://doi.org/10.1016/j.electacta.2011.07.017

[10] Wijesundera, R. P. "Fabrication of the CuO/Cu2O heterojunction using an electrodeposition technique for solar cell applications." Semiconductor science and technology 25, no. 4 (2010): 045015. https://doi.org/10.1088/0268-1242/25/4/045015

[11] Tran, Man Hieu, Jae Yu Cho, Soumyadeep Sinha, Myeng Gil Gang, and Jaeyeong Heo. "Cu2O/ZnO heterojunction thin-film solar cells: the effect of electrodeposition condition and thickness of Cu2O." Thin Solid Films 661 (2018): 132-136. https://doi.org/10.1016/j.tsf.2018.07.023

[12] Messaoudi, Olfa, Sarra Elgharbi, Amira Bougoffa, Moufida Mansouri, Afrah Bardaoui, Safa Teka, Leila Manai, and Arwa Azhary. "Annealing temperature investigation on electrodeposited Cu2O properties." Phase Transitions 93, no. 10-11 (2020): 1089-1099. https://doi.org/10.1080/01411594.2020.1837379

[13] Zang, Zhigang. "Efficiency enhancement of ZnO/Cu2O solar cells with well oriented and micrometer grain sized Cu2O films." Applied Physics Letters 112, no. 4 (2018).

[14] Lachinov, Alexey N., Danfis D. Karamov, Azat F. Galiev, Alexey A. Lachinov, Azat R. Yusupov, Vera V. Shaposhnikova, Sergey N. Salazkin, and Alla B. Chebotareva. "The Effect of Local Doping of the Polymer–Polymer Interface Using Cu2O Particles." Applied Sciences 13, no. 6 (2023): 3684. https://doi.org/10.3390/app13063684

[15] Sliti, Naama, Emile Fourneau, Thomas Ratz, Saâd Touihri, and Ngoc Duy Nguyen. "Mg-doped Cu2O thin films with enhanced functional properties grown by magnetron sputtering under optimized pressure conditions." Ceramics International 48, no. 16 (2022): 23748-23754. https://doi.org/10.1016/j.ceramint.2022.05.028

[16] Yuan, Binxia, Xiaobo Liu, Xiaodong Cai, Xinyi Fang, Jianfeng Liu, Maoliang Wu, and Qunzhi Zhu. "Preparation of zinc and cerium or both doped Cu2O photoelectric material via hydrothermal method." Solar Energy 196 (2020): 74-79. https://doi.org/10.1016/j.solener.2019.11.093

[17] Sliti, Naama, Emile Fourneau, Thomas Ratz, Saâd Touihri, and Ngoc Duy Nguyen. "Mg-doped Cu2O thin films with enhanced functional properties grown by magnetron sputtering under optimized pressure conditions." Ceramics International 48, no. 16 (2022): 23748-23754. https://doi.org/10.1016/j.ceramint.2022.05.028

[18] Mikrajuddin, A., and Khairurrijal Khairurrijal. "Derivation of Scherrer relation using an approach in basic physics course." (2008): 28-32.

[19] Zamzuri, Mohd, Junji Sasano, Fariza Binti Mohamad, and Masanobu Izaki. "Substrate type< 111>-Cu2O/< 0001>-ZnO photovoltaic device prepared by photo-assisted electrodeposition." Thin Solid Films 595 (2015): 136-141. https://doi.org/10.1016/j.tsf.2015.10.054

[20] Yathisha, R. O., and Y. Arthoba Nayaka. "Structural, optical and electrical properties of zinc incorporated copper oxide nanoparticles: doping effect of Zn." Journal of materials science 53 (2018): 678-691. https://doi.org/10.1007/s10853-017-1496-5

[21] Kardarian, Kasra, Daniela Nunes, Paolo Maria Sberna, Adam Ginsburg, David A. Keller, Joana Vaz Pinto, Jonas Deuermeier et al. "Effect of Mg doping on Cu2O thin films and their behavior on the TiO2/Cu2O heterojunction solar cells." Solar Energy Materials and Solar Cells 147 (2016): 27-36. https://doi.org/10.1016/j.solmat.2015.11.041

[22] Mukherjee, Indrani, Sriparna Chatterjee, and Nilesh A. Kulkarni. "Band gap tuning and room-temperature photoluminescence of a physically self-assembled Cu2O nanocolumn array." The Journal of Physical Chemistry C 120, no. 2 (2016): 1077-1082. https://doi.org/10.1021/acs.jpcc.5b10597

[23] Elfadill, Nezar G., M. R. Hashim, Khaled M. Chahrour, and S. A. Mohammed. "Preparation of p-type Na-doped Cu2O by electrodeposition for a pn homojunction thin film solar cell." Semiconductor Science and Technology 31, no. 6 (2016): 065001. https://doi.org/10.1088/0268-1242/31/6/065001

[24] Nyborg, Martin, Alexander Azarov, Kristin Bergum, and Eduard Monakhov. "Deposition and characterization of lithium doped direct current magnetron sputtered Cu2O films." Thin Solid Films 722 (2021): 138573. https://doi.org/10.1016/j.tsf.2021.138573

[25] Zhiyun Zhang, Chonggao Bao, Wenjing Yao, Shengqiang Ma, Lili Zhang, Shuzeng Hou. "Superlattices and Microstructures Influence of deposition temperature on the crystallinity of Al-doped ZnO thin films at glass substrates prepared by RF magnetron sputtering method," Superlattices Microstruct. 49, no. 6 (2011): 644–653. https://doi.org/10.1016/j.spmi.2011.04.002

[26] Lai, Guozhong, Yangwei Wu, Limei Lin, Yan Qu, and Fachun Lai. "Low resistivity of N-doped Cu2O thin films deposited by rf-magnetron sputtering." Applied surface science 285 (2013): 755-758. https://doi.org/10.1016/j.apsusc.2013.08.122